

Effects of nitrogen pressure on microstructures and properties of $\text{Sr}_2\text{Fe}_{10/9}\text{Mo}_{8/9}\text{O}_6$ thin films

Jie Xu, Wei-Jing Ji, Jing-Feng Wang, Zheng-Bin Gu*, Shan-Tao Zhang*

National Laboratory of Solid State Microstructure and Department of Materials Science and Engineering, Nanjing University, Nanjing 210093, China

Received 29 July 2013; received in revised form 28 August 2013; accepted 28 August 2013

Available online 4 September 2013

Abstract

High quality double perovskite $\text{Sr}_2\text{Fe}_{10/9}\text{Mo}_{8/9}\text{O}_6$ thin films have been prepared on (111)- SrTiO_3 substrates under different N_2 partial pressures (0.1–20 Pa). The films are (111)-oriented with flat surfaces and sharp film/substrate interfaces. The epitaxy and local Fe/Mo ordering are revealed by high resolution transmission electron microscopy and selected area electron diffraction. It is established that the N_2 pressure has significant effects on structures and properties: With increasing N_2 pressure, the film thickness decreases and the strain increases, while the magnetization decreases monotonously. Interestingly, all the films show semiconductor-like behavior in the whole measuring temperature range but the resistivity increases with increasing N_2 pressure. The observed results are attributed to that N_2 pressure can affect the strain and the concentration of Fe–O–Mo, both play important roles in magnetic interaction, and thus affect the magnetic and transport behaviors.

© 2013 Elsevier Ltd and Techna Group S.r.l. All rights reserved.

Keywords: A. Films; Double perovskite; Ferromagnetism; Microstructure

1. Introduction

Ferromagnetic double perovskites have been extensively studied due to their fascinating fundamental physics and their potential for applications in devices such as spintronics, magnetic sensors, etc. [1,2]. These oxides can show high Curie temperature (T_c), good magnetic and transport properties even at room temperature (RT). As a typical example for ferromagnetic double perovskite, half-metal $\text{Sr}_2\text{FeMoO}_6$ (SFMO) has T_c of 420 K and magnetoresistance (MR) of -10% at RT [2,3]. Theoretically, SFMO has a net magnetization of $4 \mu_B/\text{formula unit (f.u.)}$, resulting from the antiferromagnetic coupling between Fe^{3+} ($3d^5$, $S=5/2$) and Mo^{5+} ($4d^1$, $S=1/2$) [2,3].

Up to now, pure SFMO and A- and/or B-site substituted SFMO have been intensively studied in both ceramic and thin film forms [3–9]. However, one of the drawbacks for SFMO-based double perovskite is that reducing atmosphere is

necessary for preparing single-phase, high quality samples. This drawback leads to both safety and cost considerations. Therefore, an alternative double perovskite composition, which can show ferromagnetism above RT and can be synthesized without reducing atmosphere, is desirable.

Recently, $\text{Sr}_2\text{Fe}_{1+x}\text{Mo}_{1-x}\text{O}_6$ ($x=1/9$), abbreviated as SFMO-1/9, is carefully designed and synthesized under relatively safe and cheap N_2 [10]. This composition is found to show ferromagnetism with T_c of 390 K and MR of -10% (10 K, 2 T external magnetic field). Additionally, different from the most reported, not well-designed off-stoichiometric $\text{Sr}_2\text{Fe}_{1+x}\text{Mo}_{1-x}\text{O}_6$, this composition can theoretically avoid intrinsic, off-stoichiometry-induced oxygen defects since it is actually the mixture of stoichiometric SFMO and stoichiometric $\text{Sr}_3\text{Fe}_2\text{MoO}_9$ (i.e., $\text{Sr}_2\text{Fe}_{4/3}\text{Mo}_{2/3}\text{O}_6$) with the ratio of 2:1.

Accordingly, SFMO-1/9 might be a promising room temperature ferromagnetic double perovskite without safety and cost considerations. Based on the work on ceramics [10], SFMO-1/9 thin films with different thicknesses have been reported [11]; however, it is noted that the atmosphere pressure during film fabricating is also one of the key factors determining the mechanical strength, microstructures, and thus macroscopic

*Corresponding authors.

E-mail addresses: zbgu@nju.edu.cn (Z.-B. Gu),
stzhang@nju.edu.cn (S.-T. Zhang).

properties [12–14]. That is to say, detailed works on the effects of depositing atmosphere pressure on structures and properties of SFMO–1/9 films are necessary to further optimize the properties. For this goal, in this paper, SFMO–1/9 films have been prepared in N_2 stream with different pressures of 0.1–20 Pa, the effects of N_2 pressure on structures and properties are discussed in detail.

2. Experimental

The SFMO–1/9 target for pulsed laser deposition (PLD) was synthesized by solid state reaction with starting materials of $SrCO_3$, Fe_2O_3 , and MoO_3 . Detailed information about target preparation can be found elsewhere [9]. The SFMO–1/9 thin films were fabricated on (111) $SrTiO_3$ (STO) substrates at 750 °C for 30 min by using the 355 nm output of a Brilliant Nd: YAG laser. During deposition, the laser repetition rate is 10/3 Hz, the pulse energy is 200 mJ, and the partial N_2 pressure varied from 0.1 to 20 Pa. After deposition, the films were *in situ* annealed in chamber for 10 min.

The structures of the films were investigated by X-ray diffraction (XRD, Rigaku Ultima III) and transmission electron microscopy (TEM, FEI Tecnai F20). The cross-sectional TEM samples were prepared by mechanical thinning and ion milling (Gatan PIPS) with 3.2 keV–4.4 keV Ar^+ ions for few hours. The magnetic and transport data were collected by using a superconductor quantum interference device (SQUID, Quantum Design, MPMS XL-7) and a physical property measurement system (PPMS, Quantum Design, 2001NUGC).

3. Results and discussion

Fig. 1 shows the X-ray θ – 2θ -scans of the films deposited at 0.1, 10, 15 and 20 Pa N_2 . As can be seen, only (222) peaks from the films and (111) peaks from the substrates are observed, indicating that the films are well (111)-oriented. Additionally, under 0.1 Pa and 10 Pa N_2 pressures, the diffraction peaks from the films are observed clearly locating

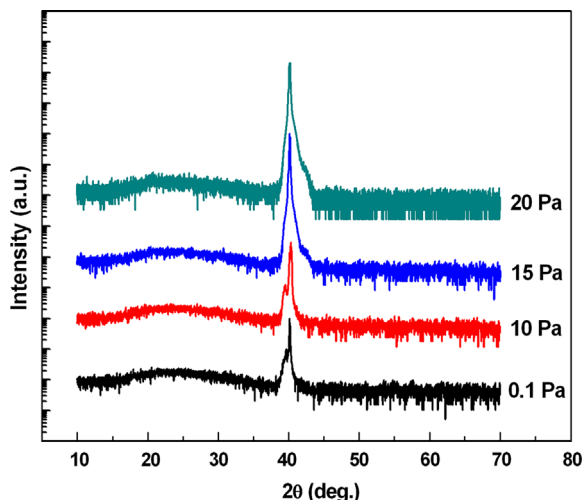


Fig. 1. X-ray diffraction patterns for the films deposited under different N_2 pressures.

left to the peaks from the substrates. The pseudocubic lattice constants are estimated to be 7.9121 and 7.8746 Å, and accordingly, the strains are estimated to be from 1.31% to 0.82%, respectively, by noting the cubic lattice constant of STO is 3.905 Å. However, when N_2 pressure is increased to 15 and 20 Pa, the peak from the films tends to combine with that from the substrates. This observation suggests that the film strain increases with increasing N_2 pressure, consistent with other report that partial pressure can lead to significant mechanical strength changing in thin films [14].

The microstructures of the films deposited at 0.1 and 15 Pa N_2 are typically investigated by TEM. The low magnification cross-sectional TEM micrographs are shown in Fig. 2(a) and (b). In general, both films are homogeneous and have very smooth surfaces and sharp film/substrate interfaces. Column-like microstructure indicates the three-dimensional growth mode, which is typical for films deposited by the PLD method. The average thickness of the films deposited at 0.1 Pa and 15 Pa N_2 is slightly different, with the values of 48 nm and 43 nm, respectively, therefore, higher the deposition pressure, smaller is the film thickness. This result is reasonable since the laser ablated compositions will have interaction with the deposition atmosphere during transporting to the substrate, higher deposition atmosphere pressure means stronger and more interactions, and thus less composition can reach the substrate to form films. Based on this TEM result, thickness of the films deposited at 10 Pa and 20 Pa N_2 are reasonably estimated to be close to 43 nm and the film thickness decreases monotonously with increasing N_2 pressure.

High resolution TEM (HRTEM) images close to the film/substrate interface for the films deposited at 0.1 and 15 Pa N_2 are taken along [011] zone-axis, as shown in Fig. 3(a) and (b), respectively. The arrows indicate the film/substrate interfaces. As can be seen, the interfaces are very sharp and the atomic arrangements across the interfaces are coherent, indicating high quality and epitaxial growth of the films.

The selected area electron diffraction (SAED) images of the films deposited at 0.1 and 10 Pa N_2 are taken from [011] zone-axis, indexed based on pseudo-cubic setting and shown in Fig. 4(a) and (b), respectively. Superlattice diffraction spots are observable, as indicated by the arrows. These superstructure reflection spots are $1/2\{h+1/2, k+1/2, l+1/2\}$, and arise from

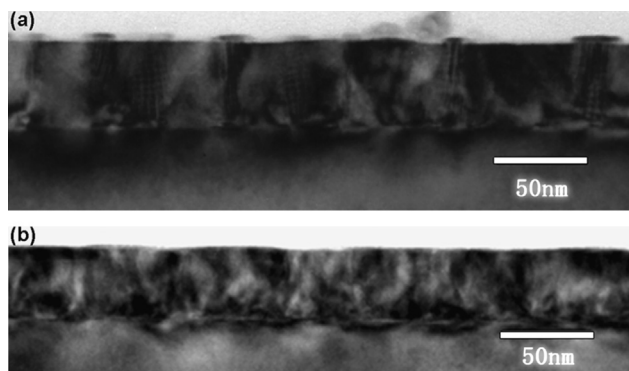


Fig. 2. The low-magnification cross-sectional TEM images of SFMO-1/9 films deposited at (a) 0.1 Pa, (b) 15 Pa N_2 pressure.

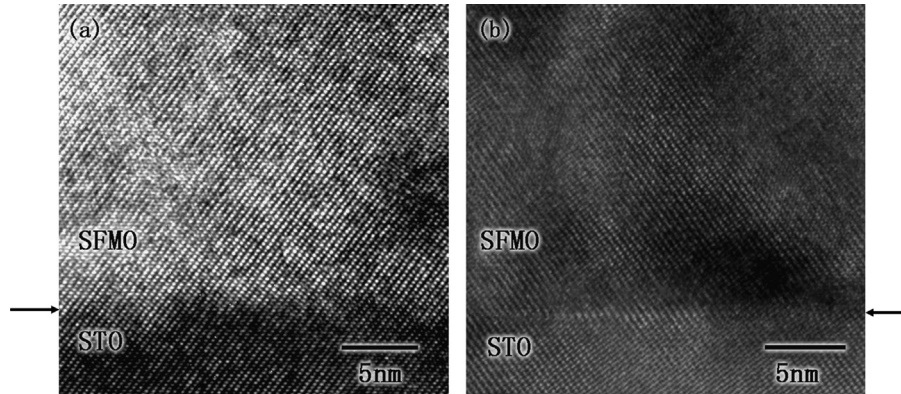


Fig. 3. HRTEM images of the interface, taken from [011] zone-axis, for the films deposited at (a) 0.1 Pa, (b) 15 Pa N_2 pressure.

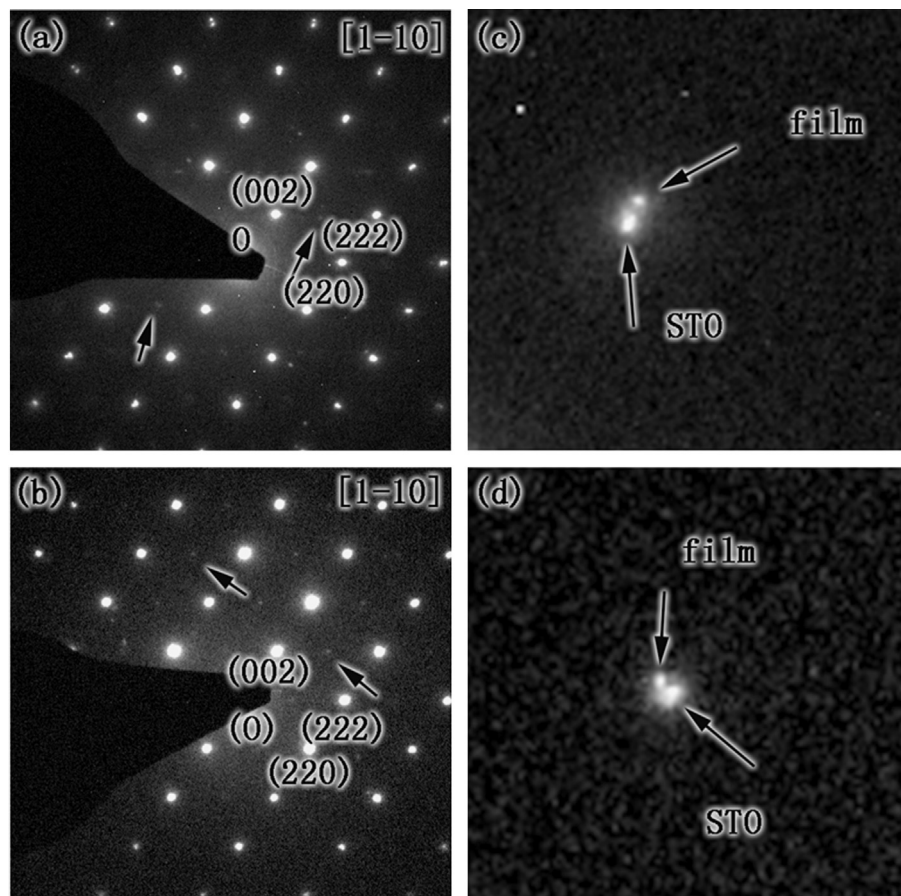


Fig. 4. SAED for the films deposited at (a) 0.1 Pa, (b) 15 Pa N_2 pressure. The enlarged diffraction spots from films and substrates show films deposited at 15 Pa N_2 (c) have higher strain than that deposited at 0.1 Pa N_2 .

the local Fe/Mo ordering which makes the unit cell twice in real space [7,15,16]. Additionally, from Fig. 4(c) and (d), it is found that the films deposited at 15 Pa have closer reflection spots from substrates and films than that deposited at 0.1 Pa N_2 , this may suggest that the films deposited under higher N_2 pressure have higher strain, consistent with the XRD results.

Magnetization-magnetic field (M – H) loops for the films deposited at 0.1, 10, 15 and 20 Pa N_2 are measured at 10 K and RT with the field of 2 T, the loops are illustrated in Fig. 5(a) and (b), respectively. In general, the films show well-saturated

M – H ferromagnetic hysteresis loops. At both temperatures, the saturation magnetization (M_s) decreases slightly with increasing N_2 pressure. For example, at 10 K, the values of M_s are 0.38, 0.35, 0.32, and 0.27 $\mu_B/f.u.$ for the films deposited at 0.1, 10, 15, and 20 Pa N_2 , respectively. As can be seen, for the films deposited under 0.1 and 10 Pa N_2 , the strain decreases from 1.31% to 0.82%, and the magnetization at 10 K decreases by 7.9% from 0.38 to 0.35 $\mu_B/f.u.$ Such pressure-dependent magnetization may be attributed to the following two factors. On the one hand, the strain increases with increasing N_2

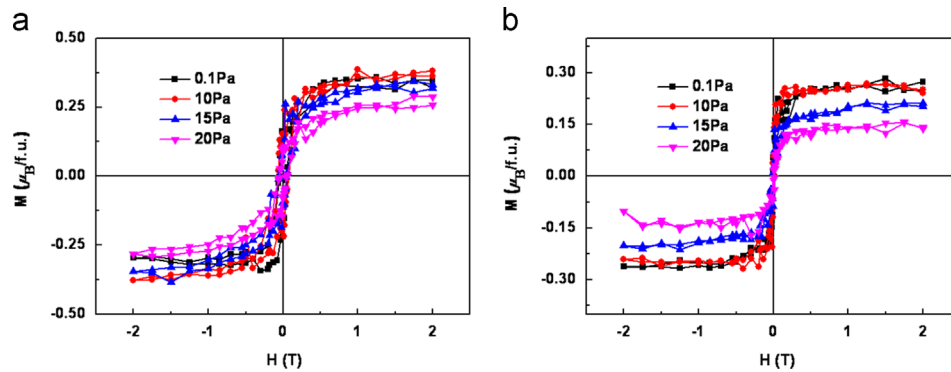


Fig. 5. M – H loops of the films at (a) 10 K and (b) 300 K.

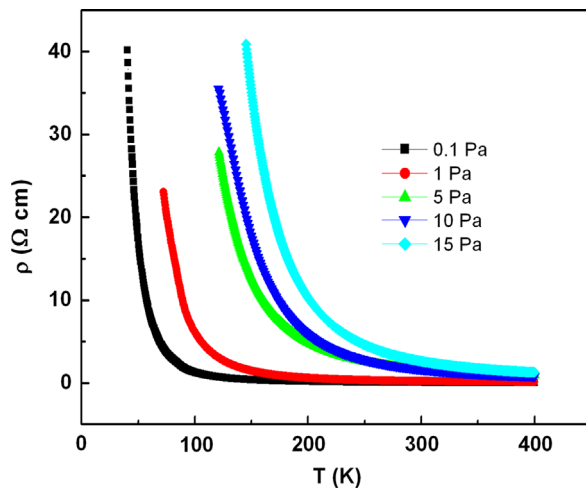


Fig. 6. Temperature dependence of resistivity of the films deposited under different N_2 pressures.

pressure, as shown in Figs. 1 and 4, the changed strain will affect the bond length and the bond angle of Fe–O–Mo. And on the other hand, some N may occupy the O sites, so N can enter into lattice, higher N_2 pressure means more substituted O by N, which might weakens the magnetic interaction by decreasing the concentration of Fe–O–Mo. These two factors can have considerable effects on magnetic interaction, and thus the macroscopic magnetic and transport behaviors [4,15,16]. To deeply understand how the strain affects bond length, bond angle, and the substituting of O by N, detailed investigating and analyzing are necessary.

From Fig. 5, it is found that the experimental magnetization value is far lower than the theoretical value ($4.0 \mu_B/\text{f.u.}$ for pure SFMO). As well known, the film thickness and the antisite disorder (ASD) play an important role in determining macroscopic magnetization value. In general thicker films and higher ASD content will lead to smaller magnetization [11]. The facts that our SFMO-1/9 should have intrinsic ASD because the Fe/Mo ratio deviates from 1:1 and the film thickness which can affect magnetic interaction as described above, should be responsible for the observed significantly low magnetization. Actually, 11 nm SFMO-1/9 films have a large magnetization of $2.3 \mu_B/\text{f.u.}$ [11].

The films deposited under 20 Pa N_2 have too large resistance to be measured. The resistances of the films deposited at 0.1, 1, 10, 15 Pa N_2 are measured and plotted in Fig. 6 as the functions of temperature. In general, all the films show semiconductor-like behavior in the whole measuring temperature range. However, the resistivity increases with increasing N_2 pressure. At 150 K, the resistivity values are 0.5, 1.7, 12.5, 17.6, and $36.1 \Omega \text{ cm}$ for the films deposited at 0.1, 1, 5, 10, and 15 Pa N_2 , respectively. Actually, this observation may be attributed to same reasons responsible for magnetization as discussed above. It is noted for the films deposited under 0.1 Pa and 10 Pa, the strain decreases from 1.31% to 0.82%; whereas the resistivity increases by 35 times from 0.5 to $17.6 \Omega \text{ cm}$, implying the significant effects of strain on transport property. Further detailed works quantifying the relationship between mechanical strength, bond length/bond angle, and magnetic/transport properties are interesting and may be helpful for further understanding the physics background.

4. Conclusions

In summary, SFMO-1/9 thin films have been prepared on SrTiO_3 (111) substrates under different N_2 pressures. The effects of N_2 partial pressure on microstructure, magnetic and transport properties have been established and discussed. It is experimentally found that with increasing N_2 pressure, the strain increases, the magnetization decreases, and the resistivity increase. These observed results are attributed to the fact that higher N_2 pressure leads to larger strain and more substituting of O by N, since the former can change the bond length and bond angle of Fe–O–Mo, while the later can decrease concentration of Fe–O–Mo, both have effect on magnetic interaction. As the results, macroscopic magnetic and transport behaviors show significant N_2 pressure dependence. Our results may be helpful for optimizing properties of ferromagnetic double perovskite thin films.

Acknowledgments

This work was supported by the National Key Basic Research Program of China (2013CB632900), the National

Nature Science Foundation of China (11174127), and the Doctoral Fund of Ministry of Education of China (201100911110014).

References

- [1] W.E. Pickett, J.S. Moodera, Half metallic magnets, *Physics Today* 54 (2001) 39–44.
- [2] D. Serrate, J.M. De Teresa, M.R. Ibarra, Double perovskites with ferromagnetism above room temperature, *Journal of Physics: Condensed Matter* 19 (2007) 023201.
- [3] K.-I. Kobayashi, T. Kimura, H. Sawada, K. Terakura, Y. Tokura, Room-temperature magnetoresistance in an oxide material with an ordered double-perovskite structure, *Nature* 395 (1998) 677–680.
- [4] G.Y. Huo, J.J. Wen, C.H. Zhang, M.H. Ren, Effect of oxygen substitution by nitrogen on magnetic and transport properties in $\text{Sr}_2\text{FeMoO}_6$ compound, *Ceramics International* 38 (2012) 1359–1363.
- [5] L. Balcells, J. Navarro, M. Bibes, A. Roig, B. Martinez, Cationic ordering control of magnetization in $\text{Sr}_2\text{FeMoO}_6$ double perovskite, *Applied Physics Letters* 78 (2001) 781–783.
- [6] D. Castro, P. Dore, R. Khasanov, H. Keller, P. Mahadevan, S. Ray, D.D. Sarma, P. Postorino, Pressure effects on the magnetic transition temperature in ordered double perovskites, *Physical Review B* 78 (2008) 184416.
- [7] A.J. Hauser, R.E.A. Williams, R.A. Ricciardo, A. Genc, M. Dixit, J.M. Lucy, P.M. Woodward, H.L. Fraser, F. Yang, Unlocking the potential of half-metallic $\text{Sr}_2\text{FeMoO}_6$ films through controlled stoichiometry and double-perovskite ordering, *Physical Review B* 83 (2011) 014407.
- [8] M. Saloaro, S. Majumdar, H. Huhtinen, P. Paturi, Absence of traditional magnetoresistivity mechanisms in $\text{Sr}_2\text{FeMoO}_6$ thin films grown on SrTiO_3 , MgO and NdGaO_3 substrates, *Journal of Physics: Condensed Matter* 24 (2012) 366003.
- [9] Y.C. Hu, H.X. Han, H.J. Hu, K.L. Zhang, H.Y. Wang, Y.J. Jiang, H. Ma, Q.F. Lu, Potassium doping effects on the structure and magnetic properties of $\text{Sr}_2\text{FeMoO}_6$, *Journal of Alloys and Compounds* 526 (2012) 1–5.
- [10] W.J. Ji, J.F. Wang, J. Xu, L. Jiao, J. Zhou, Y.B. Chen, Z.B. Gu, S.H. Yao, S.T. Zhang, Y.F. Chen, Structures, chemical states and properties of $\text{Sr}_2\text{Fe}_{1+x}\text{Mo}_{1-x}\text{O}_6$ ceramics sintered in N_2 , *Journal of Physics D: Applied Physics* 46 (2013) 015001.
- [11] W.J. Ji, J. Xu, S.T. Zhang, Y.B. Chen, J. Zhou, Z.B. Gu, S.H. Yao, Y.F. Chen, Thickness dependent microstructures and properties of $\text{Sr}_2\text{Fe}_{10/9}\text{Mo}_{8/9}\text{O}_6$ films grown in N_2 , *Solid State Communications* 163 (2013) 28–32.
- [12] S.Q. Wang, H.Y. Pan, X.P. Zhang, G.J. Lian, G.C. Xiong, Double-perovskite $\text{Sr}_2\text{FeMoO}_6$ epitaxial films with ordered cation structure grown in mixture gas of hydrogen and argon, *Applied Physics Letters* 88 (2006) 121912.
- [13] J. Orna, L. Morellon, P.A. Algarabel, J.A. Pardo, C. Magen, M. Varela, S.J. Pennycook, J.M. De Teresa, M.R. Ibarra, Growth of $\text{Sr}_2\text{CrReO}_6$ epitaxial thin films by pulsed laser deposition, *Journal of Magnetism and Magnetic Materials* 322 (2010) 1217–1220.
- [14] Ph.V. Kiryukhantsev-Korneev, J.F. Pierson, M.I. Petrzhik, M. Alnot, E.A. Levashov, D.V. Shtansky, Effect of nitrogen partial pressure on the structure, physical and mechanical properties of CrB_2 and Cr-B-N films, *Thin Solid Films* 517 (2009) 2675–2680.
- [15] J. Chang, K. Lee, M.H. Jung, J.-H. Kwon, M. Kim, S.-K. Kim, Emergence of room-temperature magnetic ordering in artificially fabricated ordered-double-perovskite $\text{Sr}_2\text{FeRuO}_6$, *Chemistry of Materials* 23 (2011) 2693–2696.
- [16] A.J. Hauser, J.R. Soliz, M. Dixit, R.E.A. Williams, M.A. Susner, B. Peters, L.M. Mier, T.L. Gustafson, M.D. Sumption, H.L. Fraser, P.M. Woodward, F.Y. Yang, Fully ordered $\text{Sr}_2\text{CrReO}_6$ epitaxial films: A high-temperature ferrimagnetic semiconductor, *Physical Review B* 85 (2012) 161201R.